Nanoscale

COMMUNICATION

Pure white-light emitting ultrasmall organic-inorganic hybrid perovskite nanoclusters

Received 00th January 20xx,
Accepted 00th January 20xx

DOI: 10.1039/x0xx00000x

www.rsc.org/

Meghan B. Teunis,[a] Katie N. Lawrence,[a] Poulami Dutta,[b] Amanda P. Siegel,[a] and Rajesh Sardar[a,*]

Organic-inorganic hybrid perovskites, direct band-gap semiconductors have shown tremendous promise for optoelectronic device fabrication. We report the first colloidal synthetic approach to prepare ultrasmall (~1.5 nm diameter), white light emitting, organic-inorganic hybrid perovskite nanoclusters. The nearly pure white-light emitting ultrasmall nanoclusters were obtained by selectively manipulating the surface chemistry (passivating ligands and surface trap-states) and controlled substitution of halide ions. The nanoclusters displayed a combination of band-edge and broadband photoluminescence properties, covering a major part of the visible region of the solar spectrum with unprecedentedly large quantum yields of ~12% and photoluninescence lifetime of ~20 ns. The intrinsic white light emission of perovskite nanoclusters makes them ideal and low cost hybrid nanomaterials for solid-state lighting applications.

The ever-increasing global demand for energy drives the need to discover highly efficient materials capable of saving energy in solid-state lighting (SSL) applications, such as light-emitting diodes (LEDs).[1,2] In this context, pure white-light emitting materials, and their subsequent uses in LED fabrication, will be a most effective way to reduce global power consumption. Currently, white-light LEDs are prepared by: (i) mixing single wavelength emitting organic phosphors,[3] and (ii) constructing multi-layer films composed of blue, green, and red color emitting semiconductor quantum dots (QDs).[4,5] However, the self-absorption process between different organic phosphors reduces device efficiency, a similar device characteristic that has also been observed for QD-based LEDs. Ultrasmall semiconductor nanoclusters (e.g., CdSe) display white-light, but they require expensive, complicated and high temperature synthetic methods.[6-8] Recently, white-light emitting bulk organic-inorganic perovskites were synthesized,[9,10] which would not only expand SSL research but also facilitate inexpensive LED fabrication.

Scheme 1. Schematic Presentation of the Synthesis of White-Light Emitting Organolead Bromide Perovskite Nanoclusters

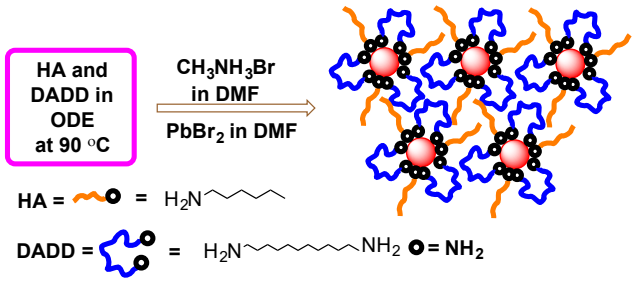

In this communication, we report the first colloidal synthetic method to prepare white-light emitting, ultrasmall (~1.5 nm diameter) methylammonium lead bromide ($MAPbBr_3$) perovskite nanoclusters (PNCs). Their synthesis is outlined in Scheme 1 and the detailed procedure is provided in the Electronic Supplementary Information (ESI) file. These PNCs display a combination of band-edge and broadband photoluminescence (PL) with a quantum yield (QY) of ~5% and PL lifetime of ~7 ns. We hypothesize that the broad emission properties originate from the presence of surface-related mid-gap trap-states. Furthermore, we showed selective manipulation of band-gap and trap-states via the preparation of mixed halide ($MAPbCl_xBr_{3-x}$) PNCs through controlled anion exchange reactions enhanced both QY and PL lifetime at least two-fold. We believe these ultrasmall PNCs will provide fundamentally important information at the molecular level because they bridge the gap between molecule-and-nanocrytals,[11] and will be a promising candidate for white light phosphors for SSL application.

[a] Department of Chemistry and Chemical Biology
Integrated Nanosystems Development Institute
Indiana University-Purdue University Indianapolis
402 N. Blackford Indianapolis, Indiana 46202, United States
E-mail: rsardar@iupui.edu
[b] Department of Chemistry
Michigan State University
578 S. Shaw Lane East Lansing, Michigan 48824, United States

Electronic supplementary information (ESI) available: Detail experimental procedure, characterizations, and figures.

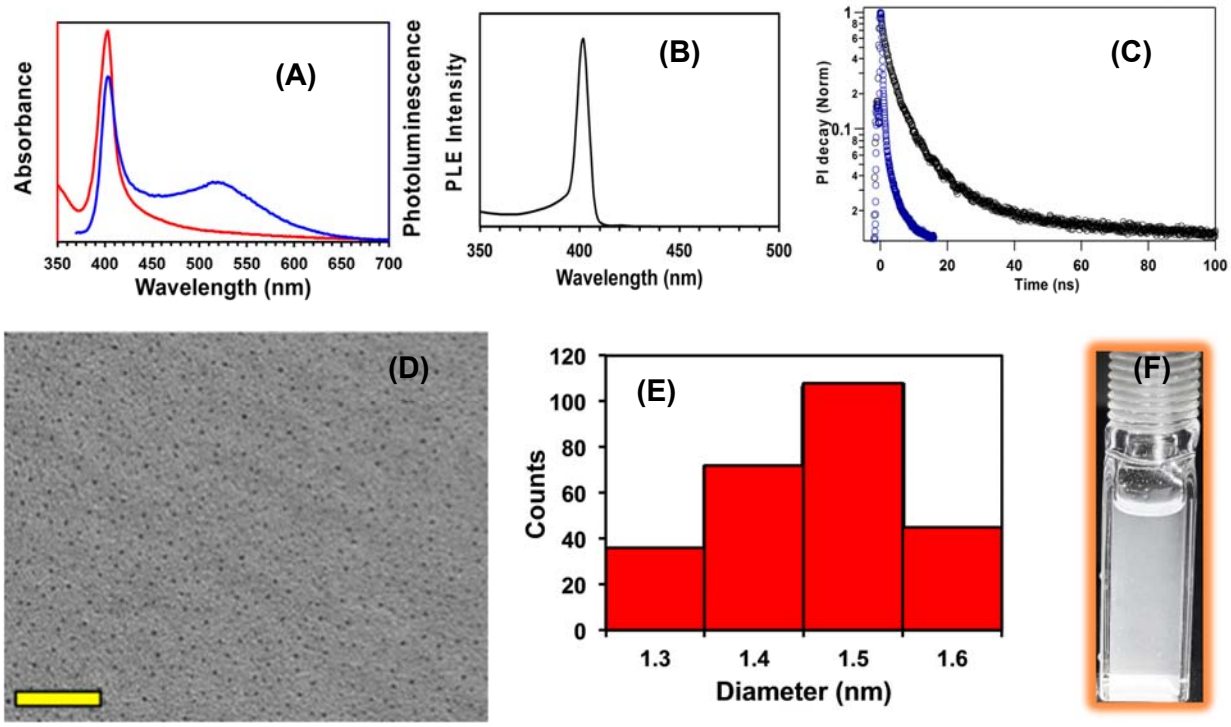

Fig. 1 (A) UV-visible absorption (red) and PL (blue) spectra of $CH_3NH_3PbBr_{3.0}$ PNCs at room temperature in toluene. The excitation wavelength was 350 nm. (B) PLE spectrum of $CH_3NH_3PbBr_{3.0}$ PNCs at room temperature in toluene. (C) PL decay traces (blue: band-edge at 409 nm; black: broad-edge at 515 nm) of the PNCs excited at 405 nm. (D) TEM image of the PNCs with 50 nm scale bar. (E) Histogram shows PNCs with an average 1.5 nm in diameter. (F) White-light emitting PNCs under illumination of UV light.

As illustrated in Fig. 1A, purified $MAPbBr_3$ PNCs in toluene display a sharp absorption peak at 402 nm. The PNCs exhibited a combination of band-edge (emission maxima at 403 nm) and broadband (emission maxima at 512 nm) PL emission that are markedly different than both organic-inorganic hybrid[12-14] and inorganic[15-18] perovskite nanocrystals, which display sharp band-edge emission features. The PLE spectrum (Fig. 1B) of the PNCs was identical in shape to that of the absorption spectrum. Therefore, our white-light PNCs have their lowest energy transition at 402 nm. The $MAPbBr_3$ PNCs display short emission lifetimes ($\tau_{band\text{-}edge}$: ~3 ns and $\tau_{broadband}$: 7 ns), see Fig. 1C. We hypothesize that the relatively longer broadband emission lifetime of our $MAPbBr_3$ PNCs in comparison to other perovskite quantum dots (QDs)[19] is associated with a combination of multi-channel radiative recombination of excitons and delocalization of excitonic wave function, as discussed later. As shown in Fig, 1D, low-resolution transmission electron microscopy (TEM) analysis of the purified PNCs showed the presence of ultrasmall nanoclusters (see Fig. 1E) with a narrow size distribution. An average diameter of 1.5 nm (see Fig. 1E) was determined from the high-resolution TEM analysis (Fig. S1). The diameter of the PNCs corresponds to only ~2 unit cells. Therefore, it was extremely difficult to capture TEM images showing lattice spacing. Exposure (5 min) of the electron beam did not damage the PNCs. The PNCs CIE chromaticity coordinates were (0.304, 0.351) (Fig. S2), which fall within the white light region of pure white light CIE coordinates of (0.333, 0.333) as perceived by the naked eye.

The sharp absorption feature indicates narrow size distribution of synthesized $MAPbBr_3$ PNCs that resemble ultrasmall CdSe nanoclusters (<2.0 nm in diameter).[20-24] A narrow size distribution would result in a sharp band-edge PL peak rather than a combination of band-edge and broadband peaks. The broad PL feature and short PL lifetimes suggest the presence of surface related trap sites in the PNCs, not their size distribution. Our organic-inorganic hybrid PNCs are coated with primary amines, which are known to be weak □-donating, L-type ligands[25] and their interaction with Pb^{2+} in PNCs would lead to formation of antibonding orbitals below the conduction band of PNCs.[26] The newly formed orbitals serve as electron trapping mid-gap states if not fully passivated, resulting in broad emission in the PL spectra. Moreover, the broad-band emission dominates because the relative number of atoms on the surface of the PNCs increases as their size decreases.[27] In this context, ultrasmall CdSe nanoclusters are known to display a combination of band-edge and broadband PL emission due to large surface to volume ratio and the presence of mid-gap trap states.[20,22,23,28,29] Therefore, the PL spectrum of our 1.5 nm diameter $MAPbBr_3$ PNCs nicely corroborate results from ultrasmall CdSe nanoclusters. We calculated PL quantum yield for the PNCs and found it to be 5%, which is at least 10-fold higher than the first generation, white-light emitting organic-lead halide bulk perovskites.[9] However, quantum yield of our PNCs is much lower than

conventional 3.3-7.0 nm diameter $MAPbBr_3$ QDs (50-70%).[12,30] It is known that the larger QDs display higher quantum yield than ultrasmall nanoclusters because of relatively fewer surface defects in the crystal structure of the QDs, which allows the majority of the exciton recombination to take place radiatively.

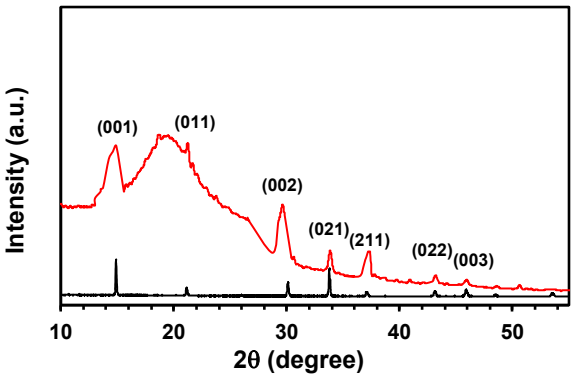

Fig. 2 X-ray diffraction (XRD) analysis of the bulk perovskite and ultrasmall PNCs. Observed XRD pattern of the bulk $MAPbBr_3$ (black) and purified ultrasmall $MAPbBr_3$ PNCs (red). The pattern of the PNCs corresponds to the cubic phase and the broadening of the diffraction peaks is characteristic of perovskite nanocrystals.[12,15]

It is important to mention that our $MAPbBr_3$ PNCs displayed approximately 90 and 120 nm blue-shifts of band-gap in comparison to $MAPbBr_3$ QDs (3.3 nm diameter)[12] and bulk[31] perovskite, respectively. Considering the relatively small exciton Bohr radius (~2.0 nm) of $MAPbBr_3$ (weak quantum confinement),[32] the observed blue shifts of PNCs were large and significant. Recent effective mass approximation (EMA) calculations by our group[33] and others[16,17,34] demonstrated that a simple spherical quantum well-based EMA calculation is not applicable to ultrasmall PNCs. A possible explanation is the potential delocalization of exciton wave functions in the strong confinement regime altering the confinement.

The energy dispersive spectroscopy (EDS) characterization (Fig. S3) showed bromide rich PNCs with Pb/Br atomic ratio of 3.8. The powder X-ray diffraction (XRD) analysis (red line) demonstrated broad peaks in comparison to the bulk perovskites (black line), two-dimensional (2D) materials,[35] and large anisotropically-shaped organolead halide perovskite nanostructures.[36] We should differentiate between our <2.0 nm diameter PNCs and 2D $MAPbBr_3$ material in terms of the Pb:Br ratio. It was reported that in 2D single-layered $MAPbBr_3$ perovskites, the Pb:Br ratio is 1:4 using a formula of $[PbBr_4]^{2-}$.[35] The XRD pattern of our $MAPbBr_3$ PNCs is similar to a literature report of small $MAPbBr_3$ nanocrystals.[12] Our ultrasmall PNCs exhibited cubic structure (Fig. 2) and thus consist of octahedral unit cells of $[PbBr_6]^{4-}$. Therefore, excess bromide ions should reside at the surface of the $MAPbBr_3$ PNCs. Our experimental data are in agreement with the literature suggesting an ~4.0 Pb/Br ratio for <2.0 nm diameter PNCs.[12] Therefore, because of higher bromide content in the structure of ultrasmall PNCs than traditional $MAPbBr_3$ perovskite, we refer to them as $MAPbBr_{3.8}$ for the rest of this communication. Furthermore, the diameter of 1.34 nm calculated using Scherrer equation (see ESI file) is close proximity to the value characterized with TEM. Appearance of the broad peak at 1.52 ppm associated with the NH_2 resonance of amine in the ^1H NMR analysis confirmed the presence of a primary amine (hexylamine (HA) and/or diaminododecane (DADD)) at the surface of the PNCs (Fig. S4). Moreover, the α and β protons that were adjacent to $–NH_2$ appearing at 2.72 and 1.6 ppm, respectively, were also broad and resembled surface attached ligands.

Although absorption spectra and white light emission under photoexcitation of our ultrasmall $MAPbBr_3$ PNCs are similar to the literature reports of bulk 2D perovskite,[9,10] atomically thin 2D perovskite,[35] and quasi-2D layered organic-$PbBr_3$ perovskite materials,[37] the physical, emission, and structural properties of our PNCs are markedly different than those 2D materials. (1) Our ultrasmall $MAPbBr_3$ PNCs are fully soluble in non-polar organic solvents such as toluene and chloroform (Fig. 1F), but 2D perovskite materials are not. Therefore, their optical characterizations of bulk and atomically thin 2D materials were conducted in solid-state[9,10,35] as oppose to our colloidal-state analysis. (2) 2D organic-$PbBr_3$ perovskite display either sharp band-edge[35,38] or broadband[9,10] PL properties, but our ultrasmall $MAPbBr_{3.8}$ PNCs display a combination of band-edge and broadband emission. (3) In addition, the diffraction peaks in our ultrasmall $MAPbBr_{3.8}$ PNCs were dramatically broadened as compared to any-type of 2D perovskites.[35,38] The XRD patterns of our PNCs are similar to the literature report of ~3.3 nm diameter $MAPbBr_3$ nanocrystals,[12] which display relatively sharper XRD peaks than our $MAPbBr_{3.8}$ PNCs, suggesting an even smaller size than the literature report of 3.3 nm diameter $MAPbBr_3$

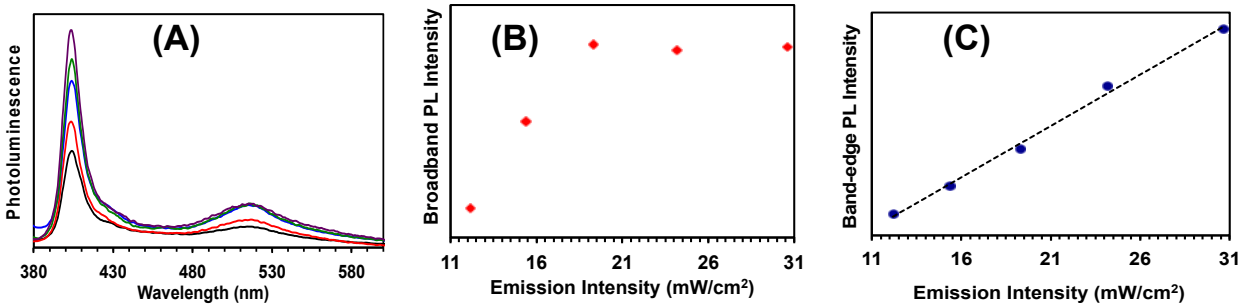

Fig. 3. (A) PL spectra of $MAPbBr_{3.8}$ PNCs at different excitation power density (mW/cm^2): black (11.2), red (15.4), blue (19.3), green (24.2), and purple (30.6). Dependence of broadband (B) and band-edge (C, $R^2 = 0.995$) PL intensity as a function of excitation power density of $MAPbBr_{3.8}$ PNCs at room temperature.

nanocrystals. Finally, synthesis of bulk or atomically thin, 2D layered organic-$PbBr_3$ perovskite requires short chain diamines as surface passivating ligands. [9,10,35] In this context, we have found that the presence of both medium chain length monoamine (HA) and long chain length diamine (DADD) in the reaction mixture is essential to obtain white-light emitting $MAPbBr_{3.8}$ PNCs. In this context, synthesis of PNCs in the absence of DADD while keeping other conditions identical resulted in insoluble bulk $MAPbBr_3$ perovskite (Fig. S5). Furthermore, absence of HA produced white-light emitting $MAPbBr_3$ PNCs but QY was found to be <0.6% (see Fig. S6 for optical and XRD characterization). Therefore, the presence of HA and DADD onto the surface of $MAPbBr_3$ PNCs is a prerequisite to keep them in their ultrasmall size regime and maintain the surface related trap-states, resulting in white-light emission.

As shown in Fig. 1A, $MAPbBr_{3.8}$ PNCs display a combination of band-edge and broadband PL properties. It is mentioned in the literature that the broad PL emission of 2D perovskite materials generally occurred from self-trapping of excitons or electrons/holes.[10,39,40] This electronic process is different than our proposed mechanism, which involves radiative recombination of excitons at mid-gap trap-states giving our broad PL peak. To unravel the exact mechanism, we performed power dependent excitation PL studies (see Fig. 3A). Importantly, the broad PL emission peak became saturated as the power was increased (Fig. 3B). Thus, the experimental data do not support the self-trapping of excitons because if this would occur the PL intensity would follow a linear relationship with excitation power.[39,40] Considering that the trap-state concentration in $MAPbBr_{3.8}$ PNCs is finite and slow to relax, trap-state PL would be expected to saturate at high excitation power, as shown for GaN.[41] Therefore, our results strongly support trap-state-related emission. Importantly and as expected, the band-edge PL peak demonstrated a linear dependence with excitation power. Taken together, our experimental data suggest that the PL properties we observed (Fig. 1A) appear solely from the ultrasmall $MAPbBr_{3.8}$ PNCs but not from a mixture of three-dimension (3D) and 2D structures. Furthermore, our optical data are in agreement with our XRD pattern that indicates ultrasmall PNCs of 3D crystal phase.

Based on the results described above, we propose that our white-light emission originates from contributions of sharp emission in the blue region and broad emission in the green region and thus is a combined effect from the large band-gap and presence of mid-gap trap states. In other words, by systematic manipulation of spectral features we should be able to control the PNCs CIE chromaticity coordinates as well as brighten the white-light emission. Therefore, our strategy to enhance these photophysical properties of $MAPbBr_{3.8}$ PNCs involves increasing exciton binding energy and/or reducing trap states. To achieve this, we performed anion exchange reactions of purified, ultrasmall $MAPbBr_{3.8}$ PNCs with methylammonium chloride (MACl). The EDS analysis (Fig. S7) confirmed the formation of mixed halide, $MAPbCl_{1.3}Br_{2.5}$ PNCs,

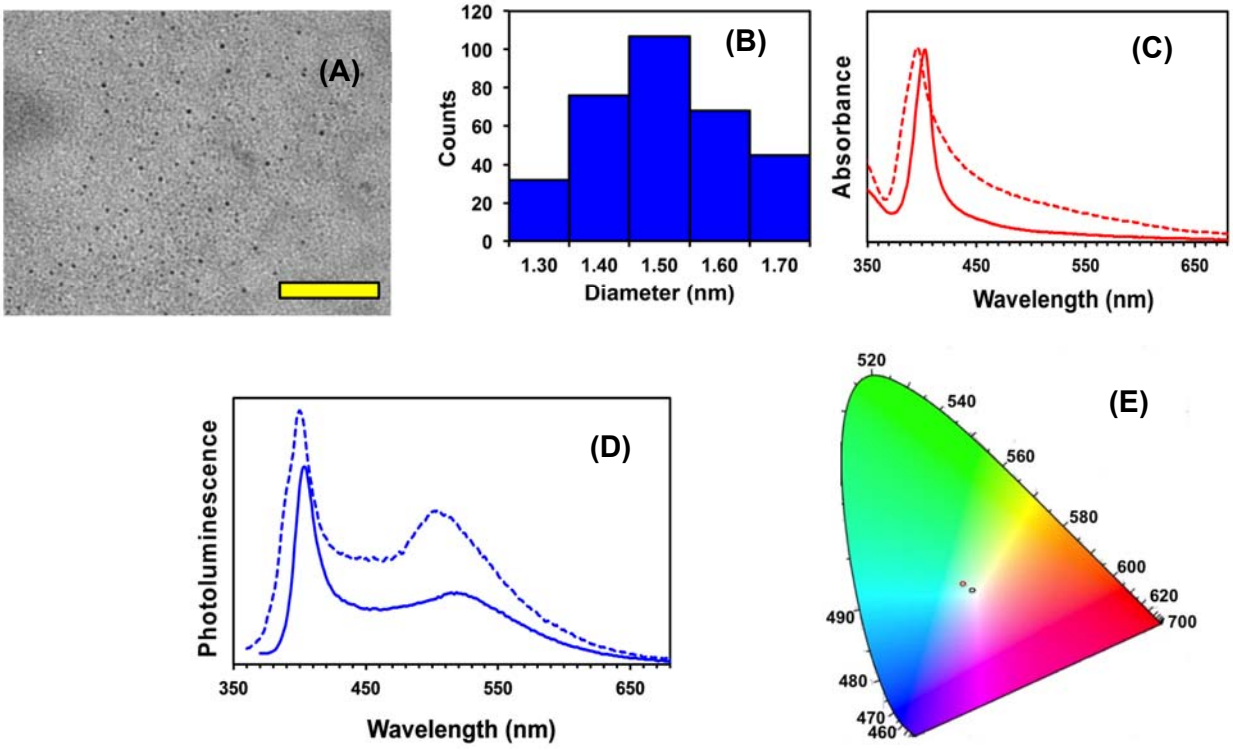

Fig. 4 (A) TEM image of the $MAPbCl_{1.3}Br_{2.5}$ PNCs. The scale bar is 50 nm. (B) Histogram for PNCs shown in panel A. (C) UV-vis spectra of $MAPbBr_{3.8}$ (solid line) and $MAPbCl_{1.3}Br_{2.5}$ (dotted line) PNCs. (D) PL spectra of $MAPbBr_{3.8}$ (solid line) and $MAPbCl_{1.3}Br_{2.5}$ (dotted line) PNCs at 350 nm excitation. (E) CIE coordinates of $MAPbBr_{3.8}$ (red) and $MAPbCl_{1.3}Br_{2.5}$ (black) PNCs.

which displayed cubic crystal structure (Fig. S8). A slight shift of the (022) plane to a higher diffraction angle in $MAPbCl_{1.3}Br_{2.5}$ PNCs in comparison to the original $MAPbBr_{3.8}$ PNCs suggests exchange of bromide ions by chloride ions. Thus, we hypothesize that the majority of the surface bromide ions, along with some octahedral unit cells of $[PbBr_6]^{4-}$ bromide ions, were exchanged with chloride ions (Fig. S9). TEM analysis confirmed no detectable change in the size of PNCs due to chloride exchange (Fig. 3A). However, due to their extremely small size, it would be difficult to accurately measure so slight a variation in the core diameter of PNCs.

Absorption measurement of our $MAPbCl_{1.3}Br_{2.5}$ PNCs showed an ~6 nm blue shift in the band-gap (Fig. 4C), which is in agreement with the EDS analysis described above and the literature that chloride substitution of both bulk organic-$PbBr_3$ perovskites[42] and $MAPbBr_3$ nanocrystals[43,44] increases the band-gap because of the stabilization of their valence band with more electronegative chloride as compared to bromide.[45] Small blue-shift is also in agreement with the suggestion that fewer octahedral unit cells of $[PbBr_6]^{4-}$ bromide ions were exchanged with chloride ions. Thus, the cubic crystal structure of the PNCs is dominated by the bromide ions. In the PL characterization (Fig. 4D), we observed changes in the position and shape of the broad-band emission in mixed halide PNCs that could suggest an influence of chloride in the excited states, which are involved in the emission properties.[10] Moreover, increase in the band-gap increases the exciton binding energy[46] that results in an enhancement of the possibility of more efficient recombination of the excitons.[27] We observed a QY up to 12% of $MAPbCl_{1.3}Br_{2.5}$ and radiative lifetimes ($\tau_{band\text{-}edge}$: ~5 ns and $\tau_{broadband}$: 19 ns) see Fig. S10. The broadband emission lifetime is more than two fold higher than $MAPbBr_{3.8}$ PNCs. Moreover, we observed nearly homogeneous emission (determined from the PL lifetime) of our $MAPbCl_{1.3}Br_{2.5}$ PNCs (data not shown). Importantly, the PLQY of our $MAPbCl_{1.3}Br_{2.5}$ nanoclusters is higher than the white-light emitting bulk organic-lead halide perovskites (PLQY = 9%).[10] The CIE chromaticity coordinates (Fig. 4E) of $MAPbCl_{1.3}Br_{2.5}$ are (0.332, 0.341) which are very close to the CIE coordinates of pure white-light. Perhaps as recently demonstrated for $CsPbBr_3$ nanocrystals,[16,47] control halide exchange and preparation of white-light emitting inorganic perovskite nanoclusters are feasible if one were able to synthesize them in their ultrasmall size regime. We should mention that prolonged chloride exchange of $MAPbBr_{3.8}$ PNCs resulted in insoluble white materials, thus demonstrating the importance of controlling the structural modification of nanoclusters to obtain desired photophysical properties.

Our structural and spectroscopic characterizations suggest that the bromide at the surface of the $MAPbBr_{3.8}$ PNCs were exchanged with chloride. Because of the higher electronegativity of chloride than bromide, surface exchange reduces the surface related radiative mid-gap trap states[48] and increases the QY and radiative lifetimes as observed previously for CdSe[28] and CdTe nanoclusters,[49] respectively. In order to further investigate the trap state-related emission, we studied the excitation wavelength dependent PL properties. Fig. 5A demonstrates the broadband emission intensity as a function of excitation wavelength of $MAPbBr_{3.8}$ and $MAPbCl_{1.3}Br_{2.5}$ PNCs. The nonlinearity in the relationship along with change in the broadband emission peak in $MAPbBr_{3.8}$ PNCs suggest the presence of variable defect sites,[50] which were not observed for $MAPbCl_{1.3}Br_{2.5}$ PNCs as a consequence of the reduction of nonradiative surface mid-gap trap states. We also observed the change in the broadband peak shape between these two PNCs (Fig. 5B), suggesting the presence of different trap sites. Another important observation we made is the increase in $\tau_{broadband}$ of $MAPbCl_{1.3}Br_{2.5}$ over that of $MAPbBr_{3.8}$ PNCs. However, one should expect the opposite effect in lifetime after chloride substitution because of the increase in confinement energy that would result in higher exciton binding energy and efficient recombination of excitons. It is reported that the kinetic energy of excitons increases as the confinement energy increases.[46,51] Under such circumstance, the excitonic wave functions could easily fill the organic-inorganic hybrid core of $MAPbCl_{1.3}Br_{2.5}$ more completely than $MAPbBr_{3.8}$ PNCs, and thus be prone to delocalize into the ligand monolayer. The delocalization of exciton wave functions increases the PL lifetime and PLQY, as recently reported for ultrasmall CdSe nanoclusters.[52] Nevertheless, further investigation is required to fully delineate the origin of the white-light emission of these ultrasmall organic-inorganic PNCs. The unique photophysical properties of these PNCs have tremendous potential for SSL applications, as we

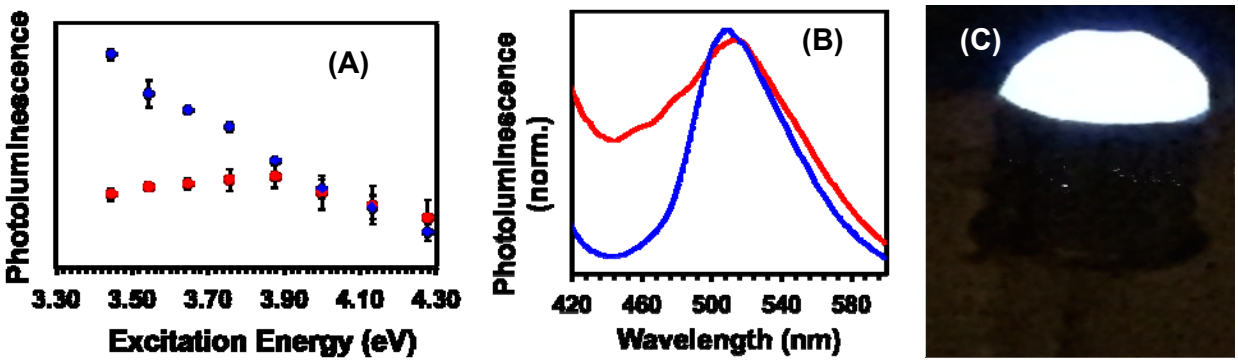

Fig. 5 (A) Excitation wavelength dependent broadband PL intensity of $MAPbBr_{3.8}$ (red) and $MAPbCl_{1.3}Br_{2.5}$ (blue) PNCs. (B) Comparison of broadband PL peak of $MAPbBr_{3.8}$ (red) and $MAPbCl_{1.3}Br_{2.5}$ (blue) PNCs at 350 nm excitation. (C) A 5 mm commercial UV LED (360 nm) coated with $MAPbCl_{1.3}Br_{2.5}$ PNCs in polyurethane.

demonstrated with a proof-of-concept white-light source fabrication using a thin coating of $MAPbCl_{1.3}Br_{2.5}$ PNCs in polyurethane (Fig. 5C).

Recently, it was reported that perovskite QDs display excellent PLQY,[12,17-19,53] high carrier mobilities, and larger diffusion lengths,[54] which are crucial electronic properties for photovoltaic applications. These electronic properties arise because of excellent passivation of the QDs surface and reduction of the nonradiative trap states. However, the very narrow band-edge emission characteristic of QDs makes it difficult to produce white light emission and fabricate LEDs for SSL applications. In this present study, we utilized surface-related trap states (defect sites) to generate a complimentory broadband emission in PNCs. The combined band-edge and broadband emissions of our PNCs cover most of the visible region of the solar spectrum, which in turn results in white-light emission. Taken together, manipulation of the appropriate amount of radiative trap states in PNCs will enhance their optoelectronic properties and facilitate their applications in white light emitting LED fabrication.

In summary, we have developed the first hybrid perovskite nanocluster synthetic method that is capable of producing nearly pure white light, thus enhancing the possibility to use these PNCs as single source materials for SSL applications. Our PNCs would provide three important beneficial features in LED fabrication in comparison to traditionally used phosphors (organic and/or inorganic) or mixtures of different light-emitting QDs: (1) Mixing of multiple single light-emitting phosphors is commonly performed to cover the entire visible region of the solar spectrum. This mixing process reduces the device efficiency because the different phosphors decompose at different rates. (2) Inorganic phosphors require metal ion doping in order to achieve white-light emission.[55,56] (3) White-light emitting multi-layer films can be prepared by mixing various color-emitting QDs but the devices suffer significant deficiency due to the self-absorption process that arises from different sized nanoclusters. Our organic-inorganic hybrid PNCs obviate all these drawbacks. Moreover, these PNCs have the potential to provide fundamentally new optical and electronic properties at the molecule-nanocrystal interface that could be utilized to maximize charge transport efficiency in optoelectronic devices.

ACKNOWLEDGMENT

We thank Muchuan Hau and Prof. R. Decca for helping with excitation energy dependent PL measurements, and Prof. B. Muhoberac for suggestions. This work was supported by the NSF under Award CBET-1604617. EDS and XRD analyses were conducted using instruments, which were purchased from NSF-MRI grant, 1229524 and 1429241, respectively.

References

1 The Promise of Solid State Lighting for General Illumination; Optoelectronics Industry Development Association: Washington, D. (2001).

2 Using Light-Emitting Diodes. 2010, http://www1.eere.energy.gov/buildings/ssl/sslbasics_ledbacics.html; **accessed Nov 2010.**

3 Tang, C.,Liu, X.-D.,Liu, F.,Wang, X.-L.,Xu, H. and Huang, W. *Macromol. Chem. Phys.*, 2013, **214**, 314-342.

4 Coe, S.,Woo, W.-K.,Bawendi, M. and Bulovic, V. *Nature*, 2002, **420**, 800-803.

5 Colvin, V. L.,Schlamp, M. C. and Alivisatos, A. P. *Nature*, 1994, **370**, 354-357.

6 Yu, K. *Adv. Mater.*, 2012, **24**, 1123-1132.

7 Harrell, S. M.,McBride, J. R. and Rosenthal, S. J. *Chem. Mater.*, 2013, **25**, 1199-1210.

8 Kim, B. H.,Hackett, M. J.,Park, J. and Hyeon, T. *Chem. Mater.*, 2013, **26**, 59-71.

9 Dohner, E. R.,Hoke, E. T. and Karunadasa, H. I. *J. Am. Chem. Soc.*, 2014, **136**, 1718-1721.

10 Dohner, E. R.,Jaffe, A.,Bradshaw, L. R. and Karunadasa, H. I. *J. Am. Chem. Soc.*, 2014, **136**, 13154-13157.

11 Cossairt, B. M. and Owen, J. S. *Chem. Mater.*, 2011, **23**, 3114-3119.

12 Zhang, F.,Zhong, H.,Chen, C.,Wu, X.-g.,Hu, X.,Huang, H.,Han, J.,Zou, B. and Dong, Y. *ACS Nano*, 2015, **9**, 4533-4542.

13 Zhu, F.,Men, L.,Guo, Y.,Zhu, Q.,Bhattacharjee, U.,Goodwin, P. M.,Petrich, J. W.,Smith, E. A. and Vela, J. *ACS Nano*, 2015, **9**, 2948-2959.

14 Schmidt, L. C.,Pertegás, A.,González-Carrero, S.,Malinkiewicz, O.,Agouram, S.,Mínguez Espallargas, G.,Bolink, H. J.,Galian, R. E. and Pérez-Prieto, J. *J. Am. Chem. Soc.*, 2014, **136**, 850-853.

15 Zhang, D.,Eaton, S. W.,Yu, Y.,Dou, L. and Yang, P. *J. Am. Chem. Soc.*, 2015, **137**, 9230-9233.

16 Akkerman, Q. A.,D'Innocenzo, V.,Accornero, S.,Scarpellini, A.,Petrozza, A.,Prato, M. and Manna, L. *J. Am. Chem. Soc.*, 2015, **137**, 10276-10281.

17 Protesescu, L.,Yakunin, S.,Bodnarchuk, M. I.,Krieg, F.,Caputo, R.,Hendon, C. H.,Yang, R. X.,Walsh, A. and Kovalenko, M. V. *Nano Lett.*, 2015, **15**, 3692-3696.

18 Swarnkar, A.,Chulliyil, R.,Ravi, V. K.,Irfanullah, M.,Chowdhury, A. and Nag, A. *Angew. Chem. Inter. Ed.*, 2015, **54**, 15424-15428.

19 Vikash Kumar, R.,Abhishek, S.,Rayan, C. and Angshuman, N. *Nanotechnology*, 2016, **27**, 325708.

20 Dolai, S.,Dutta, P.,Muhoberac, B. B.,Irving, C. D. and Sardar, R. *Chem. Mater.*, 2015, **27**, 1057-1070.

21 Dolai, S.,Nimmala, P. R.,Mandal, M.,Muhoberac, B. B.,Dria, K.,Dass, A. and Sardar, R. *Chem. Mater.*, 2014, **26**, 1278-1285.

22 Wang, Y.,Zhang, Y.,Wang, F.,Giblin, D. E.,Hoy, J.,Rohrs, H. W.,Loomis, R. A. and Buhro, W. E. *Chem. Mater.*, 2014, **26**, 2233-2243.

23 Bowers, M. J.,McBride, J. R. and Rosenthal, S. J. *J. Am. Chem. Soc.*, 2005, **127**, 15378-15379.

24 Lawrence, K. N.,Johnson, M. A.,Dolai, S.,Kumbhar, A. and Sardar, R. *Nanoscale*, 2015, **7**, 11667-11677.

25 Anderson, N. C.,Hendricks, M. P.,Choi, J. J. and Owen, J. S. *J. Am. Chem. Soc.*, 2013, **135**, 18536-18548.

26 Knowles, K. E.,Tice, D. B.,McArthur, E. A.,Solomon, G. C. and Weiss, E. A. *J. Am. Chem. Soc.*, 2009, **132**, 1041-1050.

27 Landes, C. F.,Braun, M. and El-Sayed, M. A. *J. Phys. Chem. B*, 2001, **105**, 10554-10558.

28 Rosson, T. E.,Claiborne, S. M.,McBride, J. R.,Stratton, B. S. and Rosenthal, S. J. *J. Am. Chem. Soc.*, 2012, **134**, 8006-8009.

29 Kasuya, A.,Sivamohan, R.,Barnakov, Y. A.,Dmitruk, I. M.,Nirasawa, T.,Romanyuk, V. R.,Kumar, V.,Mamykin, S. V.,Tohji, K.,Jeyadevan, B.,Shinoda, K.,Kudo, T.,Terasaki, O.,Liu, Z.,Belosludov, R. V.,Sundararajan, V. and Kawazoe, Y. *Nat. Mater.*, 2004, **3**, 99-102.

30 Gonzalez-Carrero, S.,Galian, R. E. and Perez-Prieto, J. *J. Mater. Chem. A*, 2015, **3**, 9187-9193.

31 Shi, D.,Adinolfi, V.,Comin, R.,Yuan, M.,Alarousu, E.,Buin, A.,Chen, Y.,Hoogland, S.,Rothenberger, A.,Katsiev, K.,Losovyj, Y.,Zhang, X.,Dowben, P. A.,Mohammed, O. F.,Sargent, E. H. and Bakr, O. M. *Science* 2015, **347**, 519-522.

32 Tanaka, K.,Takahashi, T.,Ban, T.,Kondo, T.,Uchida, K. and Miura, N. *Solid State Commun.*, 2003, **127**, 619-623.

33 Teunis, M. B.,Jana, A.,Dutta, P.,Johnson, M. A.,Mandal, M.,Muhoberac, B. B. and Sardar, R. *Chem. Mater.*, 2016, **28**, 5043-5054.

34 Sichert, J. A.,Tong, Y.,Mutz, N.,Vollmer, M.,Fischer, S.,Milowska, K. Z.,García Cortadella, R.,Nickel, B.,Cardenas-Daw, C.,Stolarczyk, J. K.,Urban, A. S. and Feldmann, J. *Nano Lett.*, 2015, **15**, 6521-6527.

35 Dou, L.,Wong, A. B.,Yu, Y.,Lai, M.,Kornienko, N.,Eaton, S. W.,Fu, A.,Bischak, C. G.,Ma, J.,Ding, T.,Ginsberg, N. S.,Wang, L.-W.,Alivisatos, A. P. and Yang, P. *Science*, 2015, **349**, 1518-1521.

36 Vybornyi, O.,Yakunin, S. and Kovalenko, M. V. *Nanoscale*, 2016, **8**, 6278-6283.

37 Yuan, Z.,Shu, Y.,Xin, Y. and Ma, B. *Chem. Commun.*, 2016, **52**, 3887-3890.

38 Yuan, Z.,Shu, Y.,Tian, Y.,Xin, Y. and Ma, B. *Chem. Commun.*, 2015, **51**, 16385-16388.
39 Yangui, A.,Garrot, D.,Lauret, J. S.,Lusson, A.,Bouchez, G.,Deleporte, E.,Pillet, S.,Bendeif, E. E.,Castro, M.,Triki, S.,Abid, Y. and Boukheddaden, K. *J. Phys. Chem. C*, 2015, **119**, 23638-23647.
40 Hu, T.,Smith, M. D.,Dohner, E. R.,Sher, M.-J.,Wu, X.,Trinh, M. T.,Fisher, A.,Corbett, J.,Zhu, X. Y.,Karunadasa, H. I. and Lindenberg, A. M. *J. Phys. Chem. Lett.*, 2016, **7**, 2258-2263.
41 Reshchikov, M. A. and Morkoç, H. *J. Appl. Phys.*, 2005, **97**, 061301.
42 Pellet, N.,Teuscher, J.,Maier, J. and Grätzel, M. *Chem. Mater.*, 2015, **27**, 2181-2188.
43 Pathak, S.,Sakai, N.,Wisnivesky Rocca Rivarola, F.,Stranks, S. D.,Liu, J.,Eperon, G. E.,Ducati, C.,Wojciechowski, K.,Griffiths, J. T.,Haghighirad, A. A.,Pellaroque, A.,Friend, R. H. and Snaith, H. J. *Chem. Mater.*, 2015, **27**, 8066-8075.
44 Jang, D. M.,Park, K.,Kim, D. H.,Park, J.,Shojaei, F.,Kang, H. S.,Ahn, J.-P.,Lee, J. W. and Song, J. K. *Nano Lett.*, 2015, **15**, 5191-5199.
45 Umebayashi, T.,Asai, K.,Kondo, T. and Nakao, A. *Phys. Rev. B*, 2003, **67**, 155405.
46 Brus, L. E. *J. Chem. Phys.*, 1984, **80**, 4403-4409.
47 Nedelcu, G.,Protesescu, L.,Yakunin, S.,Bodnarchuk, M. I.,Grotevent, M. J. and Kovalenko, M. V. *Nano Lett.*, 2015, **15**, 5635-5640.
48 Schreuder, M. A.,McBride, J. R.,Dukes, A. D.,Sammons, J. A. and Rosenthal, S. J. *J. Phys. Chem. C*, 2009, **113**, 8169-8176.
49 Califano, M. *ACS Nano*, 2015, **9**, 2960-2967.
50 Hoy, J.,Morrison, P. J.,Steinberg, L. K.,Buhro, W. E. and Loomis, R. A. *J. Phys. Chem. Lett.*, 2013, **4**, 2053-2060.
51 Frederick, M. T.,Amin, V. A.,Cass, L. C. and Weiss, E. A. *Nano Lett.*, 2011, **11**, 5455-5460.
52 Lawrence, K. N.,Dutta, P.,Nagaraju, M.,Teunis, M. B.,Muhoberac, B. B. and Sardar, R. *J. Am. Chem. Soc.*, 2016, **DOI: 10.1021/jacs.6b04888**.
53 Gonzalez-Carrero, S.,Espallargas, G. M.,Galian, R. E. and Perez-Prieto, J. *J. Mater. Chem. A*, 2015, **3**, 14039-14045.
54 Yettapu, G. R.,Talukdar, D.,Sarkar, S.,Swarnkar, A.,Nag, A.,Ghosh, P. and Mandal, P. *Nano Lett.*, 2016, **16**, 4838-4848.
55 Ki, W. and Li, J. *J. Am. Chem. Soc.*, 2008, **130**, 8114-8115.
56 Sun, C.-Y.,Wang, X.-L.,Zhang, X.,Qin, C.,Li, P.,Su, Z.-M.,Zhu, D.-X.,Shan, G.-G.,Shao, K.-Z.,Wu, H. and Li, J. *Nat. Commun.*, 2013, **4**, 1-7.

TOC

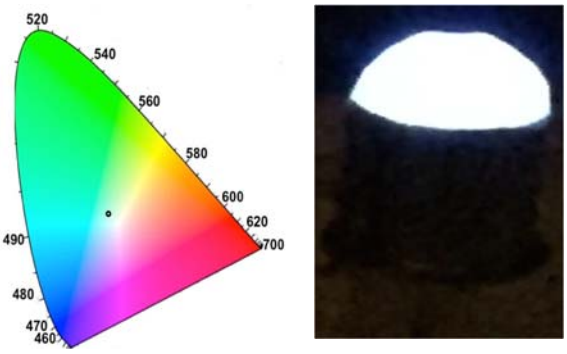

Pure white-light emitting ultrasmall organic-inorganic hybrid perovskite nanoclusters were synthesized through a simple colloidal approach. Their emission properties were controlled by manipulating the surface chemistry.